


RESEARCH

Open Access



An emerging role of microplastics in the etiology of lung ground glass nodules

Qiqing Chen^{1*†} , Jiani Gao^{2†}, Hairui Yu¹, Hang Su², Yan Yang¹, Yajuan Cao^{3,4}, Qun Zhang¹, Yijiu Ren², Henner Hollert⁵, Huahong Shi¹, Chang Chen^{2*} and Haipeng Liu^{3,4*}

Abstract

Background: Microplastic pollution has become a serious global environmental threat. The abundance of microplastics in the air is an order of magnitude higher than that in other media, which means that all living animals breathing with lungs (including humans) cannot escape the fate of inhaling microplastics. However, there is no direct evidence to demonstrate what type and abundance of microplastics exist in lung tissue. In addition, whether the retention of microplastics and the long-term friction between microplastics and lung tissue are related to some respiratory diseases is largely unknown. Ground glass nodules (GGNs) are areas of lesions of homogeneous density and with hazy increase in density in the lung field that do not obscure the bronchovascular structure, which have been increasingly identified in past decades. Although their etiology is broad, the correlation of microplastics with GGNs remains elusive.

Results: In this study, we identified the presence of 65 microfibrils, including 24 microplastics (> 20 μm) in 100 human lung tissues with μ-FTIR. The detection rate of microfibrils in tumor was 58%, higher than that in normal tissue (46%), and 2/3 of microplastics were found in tumor. Microfibrils seemed to be embedded in lung tissues, which was suggested by the in situ observation via LDIR. Additionally, sub-micron-sized plastic particles were also detected in some lung tissues with Raman. The abundance of microfibrils in lung tissue gradually accumulated with the increase of age. Moreover, the detection rate in tumor of patients with higher microfiber exposure risk history was significantly higher than those with a relatively lower one, implying microfiber inhalation could be related to the formation of GGN. Further, serious wear surface of microfibrils isolated from lung tissue emphasized a possible link of surface roughness to the disease progression.

Conclusions: Collectively, the existence of microplastics in human lung tissues was validated, and their correlation with GGN formation was preliminarily explored, which laid a foundation for future research on microplastic exposure in the etiology of lung cancer and other related respiratory diseases.

Keywords: Fibrous microplastics, Ground glass nodules, Exposure risk, Surface roughness

*Correspondence: chenqiqing@sklec.ecnu.edu.cn; changchenc@tongji.edu.cn; haipengliu@tongji.edu.cn

†Qiqing Chen and Jiani Gao have contributed equally to this work

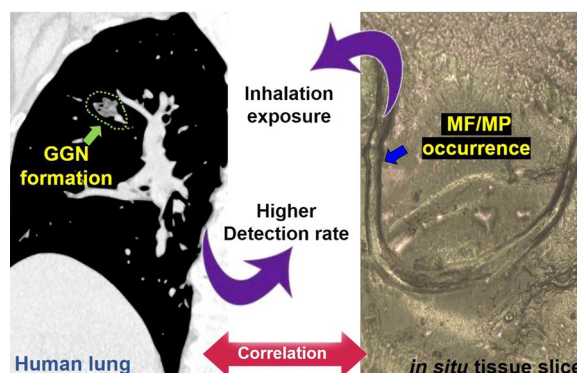
¹ State Key Laboratory of Estuarine and Coastal Research, East China Normal University, Shanghai 200241, China

² Department of Thoracic Surgery, Shanghai Pulmonary Hospital, Tongji University, Shanghai 200433, China

³ Clinical and Translational Research Center, Shanghai Pulmonary Hospital, Tongji University, Shanghai 200433, China

Full list of author information is available at the end of the article

Graphical Abstract



Introduction

Microplastic was firstly proposed as a marine environmental problem, but with its widespread occurrence in freshwater and estuary [1–3], land and mountains [4, 5], and in glaciers and polar regions [6, 7], microplastic pollution has become a global health issue and aroused some debates among scientists [8–10]. Recently, the pervasiveness of microplastics has also been verified in both indoor and outdoor air environments [11], and the human body burden of microplastics through inhalation $(0\text{--}3.0) \times 10^7$ items/year is orders of magnitude higher than that through table salt $(0\text{--}7.3) \times 10^4$ items/year or drinking water $(0\text{--}4.7) \times 10^3$ items/year [12]. This means all living animals breathing with lungs (including humans) cannot escape the fate of inhaling microplastics.

Although the inhalation of mineral fiber, such as asbestos, has been widely recognized [13, 14], pulmonary retention of non-mineral fibers, including artificial fibrous microplastics or natural cotton fibers which are difficult to be degraded due to their stable structure, remains unclear. The amount of microplastics humans take in through respiration may be much higher than other routes since microplastics are dominant in the air [12]. It has been predicted that the amount of microplastics inhaled by human body through breathing was dozens to hundreds per day [15, 16]. An early preliminary study published in 1998 reported the presence of fibers in human lung and found more inhaled fibers were present in malignant lung specimens (97%) than those in non-neoplastic ones (83%); however, there was a lack of detailed characterization of the fibers, including the size and type, color, and morphology [17]. Of note, there is no direct evidence to demonstrate what type and abundance of microplastics exist in lung tissue. In addition, whether

the retention of microplastics and the long-term friction between microplastics and lung tissue are related to some respiratory diseases is largely unknown.

Pulmonary ground glass nodules (GGNs) are areas of lesions of homogeneous density and with hazy increase in density in the lung field that do not obscure the bronchovascular structure as identified on low-dose computed tomography [18–20]. Their etiology is broad and the presumed significance is highly dependent on the underlying disease context [21, 22]. In addition to diagnostic techniques to increase the detection rate, the main causes of GGNs include genetic factors and gender factors [23–26], but research suggests that environmental factors may affect the occurrence of GGNs [24, 27, 28]. When exposed to asbestos, vinyl chloride, or other environmental factors, these substances can be inhaled into the lungs to mount an immune response. The inflammatory response may form GGNs by wrapping, organizing, or forming granulomas [27]. Additionally, a long time exposure to a dusty environment without proper protection has been reported to impair lung function and cause GGNs [28]. Moreover, people who maintain smoking habits for a long time are more likely to cause GGNs [24, 29]. The proportion of plastics produced and used in the current industrial civilization has increased year by year, leading to the existence of a large number of microplastics in the environment [1, 3, 30]. This trend is consistent with the increasing incidence of GGN in recent years especially in Asia [31], where the plastic production also ranks first (51%) worldwide [32]. In this study, we hypothesize that microplastics can contribute to the formation of GGNs. Thus, we systematically detected and characterized the microfibrils and microplastics in GGNs and

adjacent normal lung tissues, and analyzed the correlation of the presence of microfibers with the occurrence of GGNs.

Materials and methods

Clinical samples

Patients who underwent VATS lobectomy/sublobectomy for non-small cell lung cancer (NSCLC) in Shanghai Pulmonary Hospital between January 2020 and December 2020 were reviewed (Additional file 1: Table S1). Included in our studies were lung specimens with ground glass nodule (GGN). Tissue wet weight was 44 ± 32 mg (mean \pm SEM values, $n = 100$). All patients received pre-operative workups, including chest computed tomography, brain magnetic resonance imaging, whole-body PET-CT, and bronchoscopy. This work has received approval for research ethics from the Institutional Review Boards of Shanghai Pulmonary Hospital and a certificate of approval is available upon request (Approval number: K21-020).

Ventilation systems were installed to limit the circulation of chemical and biological pollutants with 20 air changes per hour. Surgeons wore white cotton sterile gowns, rubber gloves, surgical masks, and head coverings. Instruments of thoracoscopy, ultrasonic scalpel, electro-surgical knife, and aspirator would touch lung tissues during the operation. But no cotton or plastic materials would come into contact with lung tissues. After the removal of lung tissues from human bodies, they were immediately placed in stainless-steel curved plates, and the tumor and normal tissues were separated using scalpels and forceps. This study was performed in accordance with the principles of the Declaration of Helsinki.

Sample digestion, observation, and identification

We used 50-mL glass bottles for tissue digestion, and 100-mm-diameter glass Petri dishes for storing and transferring filter membranes. All glassware was thoroughly cleaned and rinsed with Milli-Q water for three times, then placed on the negative pressure ultra-clean bench, and buckled on the clean dust-free paper. After natural air drying, each lung tissue was quickly transferred from cryotubes to glass bottles with stainless-steel tweezers, together with 30 mL of 30% H_2O_2 , and immediately covered with aluminum foil. The glass bottles were then transported to an orbital shaker (ZWF-1112, Shanghai Zhicheng Co., China) for 72 h incubation with 80 rpm at 65 °C.

After tissue digestion, we quickly filtered each digested sample through a 5- μ m filter membrane (MCE, SMWP04700, Millipore, USA), which was then immediately transferred to a covered glass Petri dish (exposure time to air: <30 s). Then, the glass Petri dishes

were transferred to an ultra-clean analytical laboratory with stainless-steel inner walls in the whole room in our Marine Plastic Pollution Research Center (East China Normal University, China).

All items larger than 20 μ m were examined under a Carl Zeiss Discovery V8 Stereo microscope (Micro Imaging GmbH, Germany) and an AxioCam digital camera to observe and photograph the substances on the surface of the membranes. The suspect items were quickly picked out onto a numbered paper one by one. The observation time for each filter membrane was strictly controlled within 2 min to avoid potential microfiber contamination via air deposition to the greatest extent. Then, the composition of each item was identified with μ -FTIR (Nicolet iN 10, Thermo Fisher) under the transmission mode. A resolution of 4 cm^{-1} with a 16^{-s} scan time was chosen for data collection. Three pairs of tumor and normal tissue samples and procedural blanks were also quantified for microfibers (<20 μ m) by Raman (Renishaw). All spectra of μ -FTIR and Raman were matched with our modified database and the result was accepted only when the matching index $\geq 70\%$ according to combined libraries of "HR Hummel Polymer and Additives," "HR Aldrich Phosphorous and Sulfur Compounds," "HR Aldrich Solvents," "HR Spectra Polymers and Plasticizers by ATR," "HR Industrial Coatings," "HR White Powders," "HR Spectra RAMAN Demo," "Synthetic Fibers by Microscope," "Natural and semi-synthetic cellulose," "Common Materials," "Wizard library," "OTC Pharmaceuticals Microscope," "NR Nicolet Sampler Library," "Organics by RAMAN Sample Library," "Georgia State Crime Lab Sample Library," and "Aldrich Condensed Phase Sample Library."

As the increment of plastic production trend is consistent with the increasing incidence of GGN in recent years [31, 32], lung tissues collected 6 years ago (the earliest available) were included as former sample controls, which were stored in cryotubes at -80 °C. The Image J software (NIH Image) was used to measure the length and width of fibers. The colors of fibers were compared with Pantone International Color Card by visual inspection.

Procedural control for microfiber contamination

From the beginning of the operation to the final microfiber detection, we performed procedural blanks throughout the whole process. There were two batches of procedural control carried out on different days (each with three parallel replicates), and thus 6 procedural blank samples in total.

During patient lung surgery operations, the environmental conditions were as follows. Ventilation systems were installed to limit the circulation of chemical and biological pollutants with 20 air changes per hour. Surgeons

wore white cotton sterile operating gowns, rubber gloves, disposable surgical masks, and head coverings. Instruments of thoracoscopy, ultrasonic scalpel, electro-surgical knife, aspirator, etc., would touch lung tissues during the operation. But no cotton or plastic materials would come into contact with lung tissues. After a lung tissue removed from a human body, it was immediately placed in a stainless-steel curved plate, and the tumor and normal tissues were separated by sterile scalpels and forceps. Procedural blanks were also conducted on these curved plates with the same duration and tools. Lung tissues and procedural blanks were then transferred into glass tubes without fixing. Then, the procedural blank samples digestion, observation, and identification processes were the same as described in Sample digestion, observation, and identification.

Only one white cotton microfiber was detected in one of the procedural blanks, and no microplastic was found in all procedural blanks. The color of the detected cotton was white, different from those found in lung tissues (whose dominant colors are blue and purple). Therefore, the contamination of microfiber and microplastic was 0.18 MF/sample and 0 MP/sample (far below that quantified in lung tissues of 0.65 ± 0.70 MF/sample and 0.24 ± 0.49 MP/sample).

SEM/EDS analysis

To understand the surface morphology and elemental composition of microfibers from lung tissues, twelve representative samples (6 each of normal and tumor tissues) were studied using scanning electron microscope (SEM) (S4800) and Cryo-SEM (Lecia EM ICE, Germany) combined with energy-dispersive X-ray spectroscopy (EDS).

To confirm the effect of transportation, digestion, observation, and identification processes on the surface morphology of microfibers, we conducted a pilot experiment by preparing two kinds of microfibers with the highest detection rate in our study (cotton and rayon) from the laboratory before and after all the above processes. Microfibers collected from indoor air in Shanghai were also collected for observation, including nine microfibers (3 each of cotton, rayon, and polyester).

Microfibers were fixed on double-sided adhesive carbon tabs on the sample stage and spray gold. High-resolution imaging was carried out by field emission SEM working at 3.0 kV and 15 μ A, and the samples were taken at a magnification of 5.00 K. Qualitative elemental compositions of six selected samples were determined by EDS working at 20.0 kV and 20 μ A.

Microfiber surface roughness measurement

The surface roughness profile of microfibers was obtained using a three-dimensional white light interferometry

optical profiler Bruker Contour GT-K. The surface of middle area of microfibers was selected for detection. The entire profile data points were recorded, and the roughness average (Ra) of the absolute values of profile heights over a given area [33] was calculated for each microfiber to evaluate their roughness, according to the standard method ASME B46.1-2009 [34].

In situ observation of microfibers

The surgical lung tissues were cut into 30 μ m slices and left untreated or treated with proteinase K (20 mg/mL) at 37 °C for 10 min. Each sample was then fixed to the microscope slide of dimension 25 mm \times 75 mm using optical adhesive. To identify the in situ presence of microfibers in lung tissues, we used the Agilent 8700 Laser Direct Infrared (LDIR) Chemical Imaging System, equipped with a quantum cascade laser (QCL) source and a single point Mercury Cadmium Telluride (MCT) detector, at Agilent Technologies Application Laboratory in Shanghai, China. Briefly, the slides were firstly put in the LDIR system, and the height of samples was automatically identified and the tissue sections were focused. Then, the LDIR analyzer rapidly scanned the sample area at 1200 cm^{-1} with 20- μ m resolution, and found targeted areas containing suspect microfibers. Next, the targeted areas were enlarged and scanned with a fine resolution of 10 μ m. Finally, the spectrum data were collected, and microfiber identification results were provided according to characteristic peaks matching.

Clinical indices

Through interviews with patients, we obtained first-hand information about the history of microfiber exposure of the patients (Additional file 1: Table S2). (1) We define people who smoke or have had a history of smoking as high risk of microfiber exposure, because cigarette butts contain various types of microfibers [35] and could be inhaled in with the smoke. (2) We define people who have a high cooking frequency at home as high risk of microfiber exposure, because long time cooking and other housework will increase the microfiber exposure [36, 37]. (3) We also inquired about the occupational background of the patients, and listed the patients who work in shoe factories, farms, construction sites, garbage cleaning, etc., as having high risks of microfiber exposure.

Statistical analysis

The microfiber or microplastic amount differences between tumor and normal tissue groups were evaluated by paired *t*-test. The microfiber exposure history and gender effects on the microfiber or microplastic

detection results were evaluated by Chi-square test. All the above analyses were performed with SPSS (SPSS, version 20.0). Figures were plotted with GraphPad Prism (GraphPad, version 8.0).

Results

Identification of microfibers in human lung tissue

To detect whether microfibers are present in human lung tissues, we collected surgically dissected human lung tissues, including GGNs and adjacent normal tissues in patients with pulmonary GGNs which are pathologically diagnosed. Pulmonary GGN can be observed in preinvasive lesions, such as atypical adenomatous hyperplasia (AAH), adenocarcinoma in situ (AIS), or in malignancies, such as minimally invasive adenocarcinoma (MIA) and lepidic-predominant invasive adenocarcinomas (LPA) [38]. By using hydrogen peroxide digestion method, we successfully isolated microfibers from the lung tissues in both tumor (Fig. 1a–e) and normal (Fig. 1f–h) tissues. The most common types of microfibers are

cotton (Fig. 1a), rayon (Fig. 1b, g), polyester (Fig. 1c, h), denim (Fig. 1f), and the representative examples are presented. Besides, we also found some kind of microfibers that rarely found in water or soil, such as phenoxy resin (Fig. 1d) and chipboard (Fig. 1e) in tumor tissues. The cotton fiber detected in one procedural blank is white colored, different from those found in lung tissues (whose dominant colors are blue and purple). For the former samples (tissues collected 6 years ago), only one blue cotton fiber was detected in two tumor tissues each, and none microplastic was detected (0.33 MF/sample and 0 MP/sample), indicating a lower frequency of detection rate than that in new samples (0.65 ± 0.70 MF/sample and 0.24 ± 0.49 MP/sample). Using Raman technology, we also detected microplastics $< 20 \mu\text{m}$ in two tumor tissues from two patients (Fig. 2). The width of polyethylene glycol was $0.8 \mu\text{m}$, which can also be termed as sub-micron plastic particles.

Most of the identified items ($> 20 \mu\text{m}$) were typical fibrous ones, which was because they were mainly

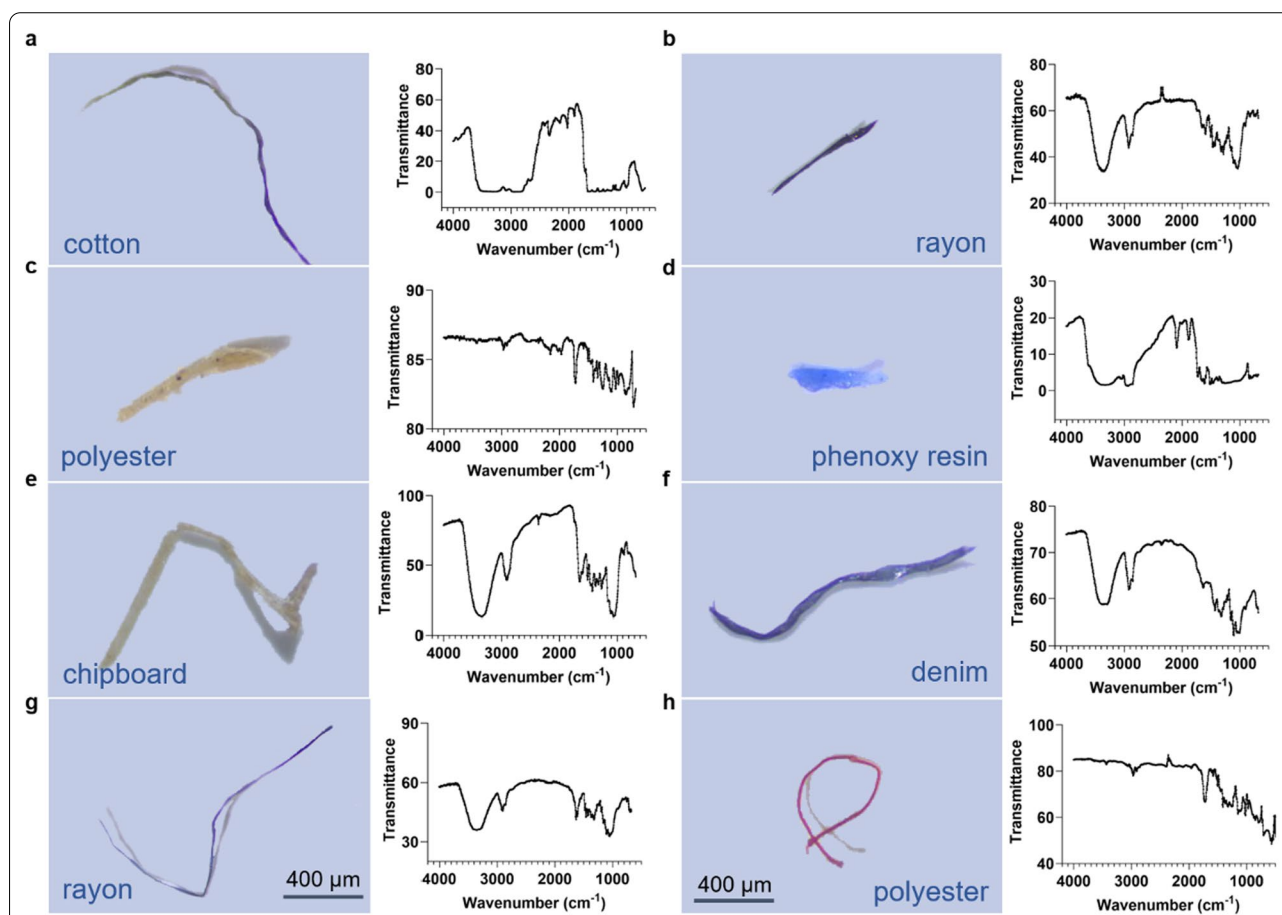
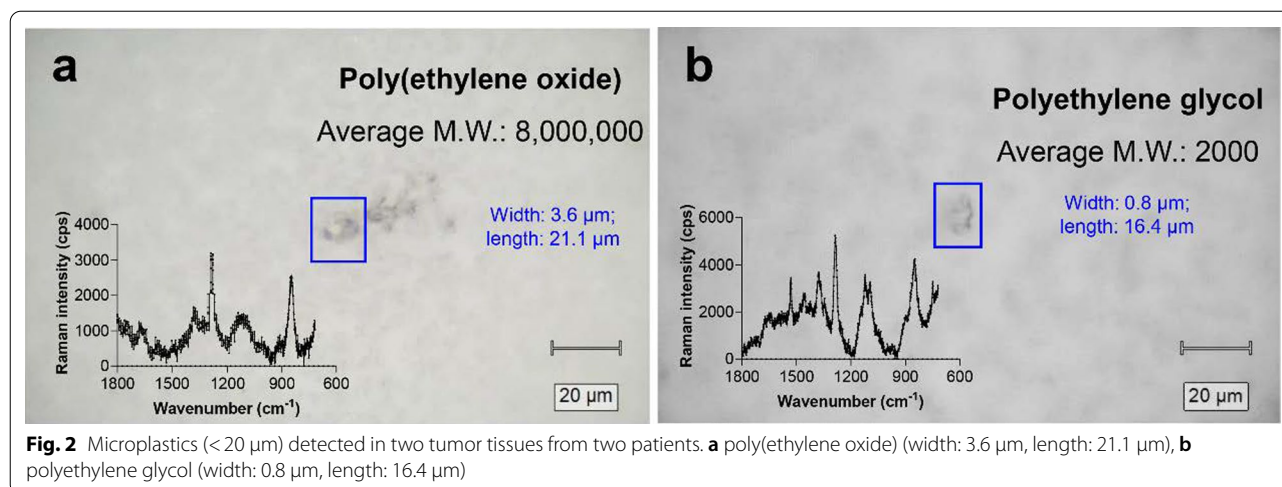


Fig. 1 Identified of microfibers (including microplastics) in human lung tissues. Images under microscope and infrared spectrum of **a** cotton in tumor tissue; **b** rayon in tumor tissue; **c** polyester in tumor tissue; **d** phenoxy resin in tumor tissue; **e** chipboard in tumor tissue; **f** denim in normal tissue; **g** rayon in normal tissue; **h** polyester in normal tissue



originated from ambient air via inhalation. It has been reported that the shape of the dominant type of fiber was > 90% of the number of particles collected in the ambient air [39]. Although some non-typical fibrous items were also found, i.e., phenoxy resin (Fig. 1d) and chipboard (Fig. 1e), they can also be characterized with length and width descriptors, like fibers, and thus, we classified them into microfibers in the present study for a unified description.

In situ detection of microfibers in human lung tissue

To further demonstrate the presence of microfibers in human lung, we employed the LDIR method to detect the microfibers in the lung tissue slice from pulmonary GGNs patients in situ. By analyzing cryo-sectioned slices, we successfully observed the presence of a microfiber (width 24 μm , length 887 μm) in the lung tissue slice by microscopy observation with both visible light (Fig. 3a, d) and infrared spectrum (Fig. 3b, c).

The infrared absorption spectrum revealed that the composition of the microfiber was cellulose (Fig. 3e). This was further consolidated by the collected signals with the specific cellulose characteristics (Fig. 3f), which indicates that this fiber component is indeed cellulose and is different from the surrounding components. As the characteristic signal intensities of this microfiber were uneven at different regions, we suppose that this microfiber should be embedded in the tissue. We therefore for the first time provide solid in situ evidence to support the presence of microfiber in human lung tissue.

Higher detection rate of microfibers in the GGNs

To understand whether the presence of microfibers is associated with the occurrence of GGNs, we further compared the frequency of the detected microfibers in

the GGNs and adjacent normal lung tissues. In 50 pairs of samples, microfibers have been found in 29 tumor and 23 normal tissues (Fig. 4a). A total of 38 microfibers were detected in tumor tissues, accounting for 58.46% of the total detected microfibers, while 27 microfibers were detected in normal tissues, accounting for 41.54% (Fig. 4b).

Among the detected microfibers, 24 were microplastics, constituting 36.92% of the total microfibers. In the female subgroup, the positive detection rates were 61.76% and 47.06% for tumor and normal tissues, respectively (Fig. 4c). In the male subgroup, the positive detection rates were 50.00% and 43.75% for tumor and normal tissues, respectively (Fig. 4d). Sixteen microplastics were detected in the tumor tissues, which was twice than that of the normal tissues. Only two types of microplastics, namely polyester and rayon, were found in normal tissues, whereas three more types of microplastics (acrylic, polyethylene glycol terephthalate (PET), and phenoxy resin) were also found in tumor tissues. Taken together, in comparison to that in normal lung tissues, the detection rate of microfibers in GGNs was higher (paired *t*-test, $t = 1.740$, $p = 0.0882$), indicating a possible link of the presence of microfibers to the occurrence of GGNs.

Characterization of microfibers in the lung tissues

We checked the characteristics, including width, length, type, and color of microfibers isolated in human lung tissues. The average values of length (mean \pm SEM values; 1.45 ± 0.98 mm) and width (35.74 ± 21.09 μm) of microfibers in tumor tissues are slightly higher than those in the normal tissues (1.38 ± 0.96 mm for length and 32.81 ± 16.91 μm for width), but there is no significant difference between them (Fig. 4a). Additionally, both the length of microplastics in tumor (1.75 ± 0.79 mm)

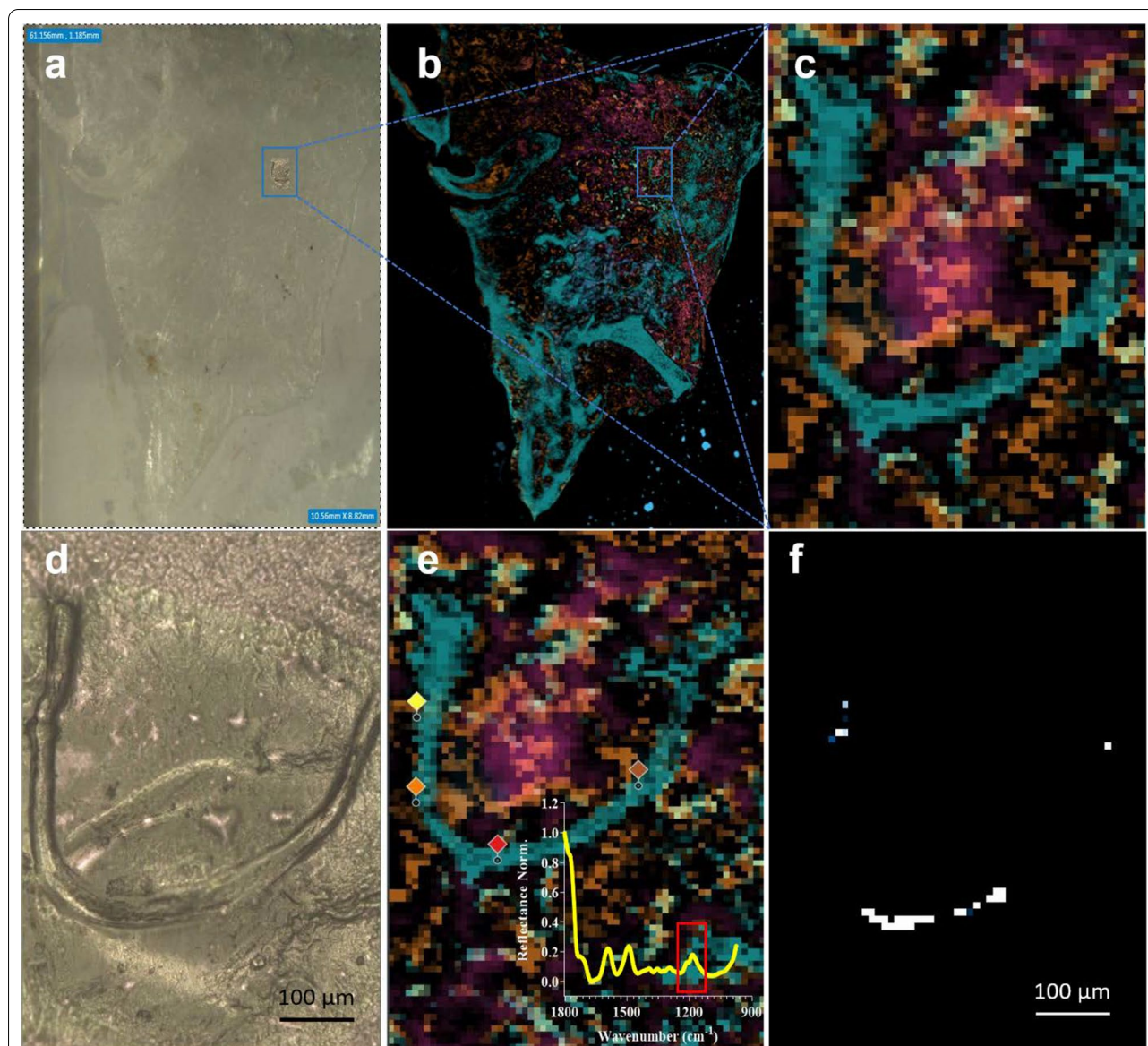
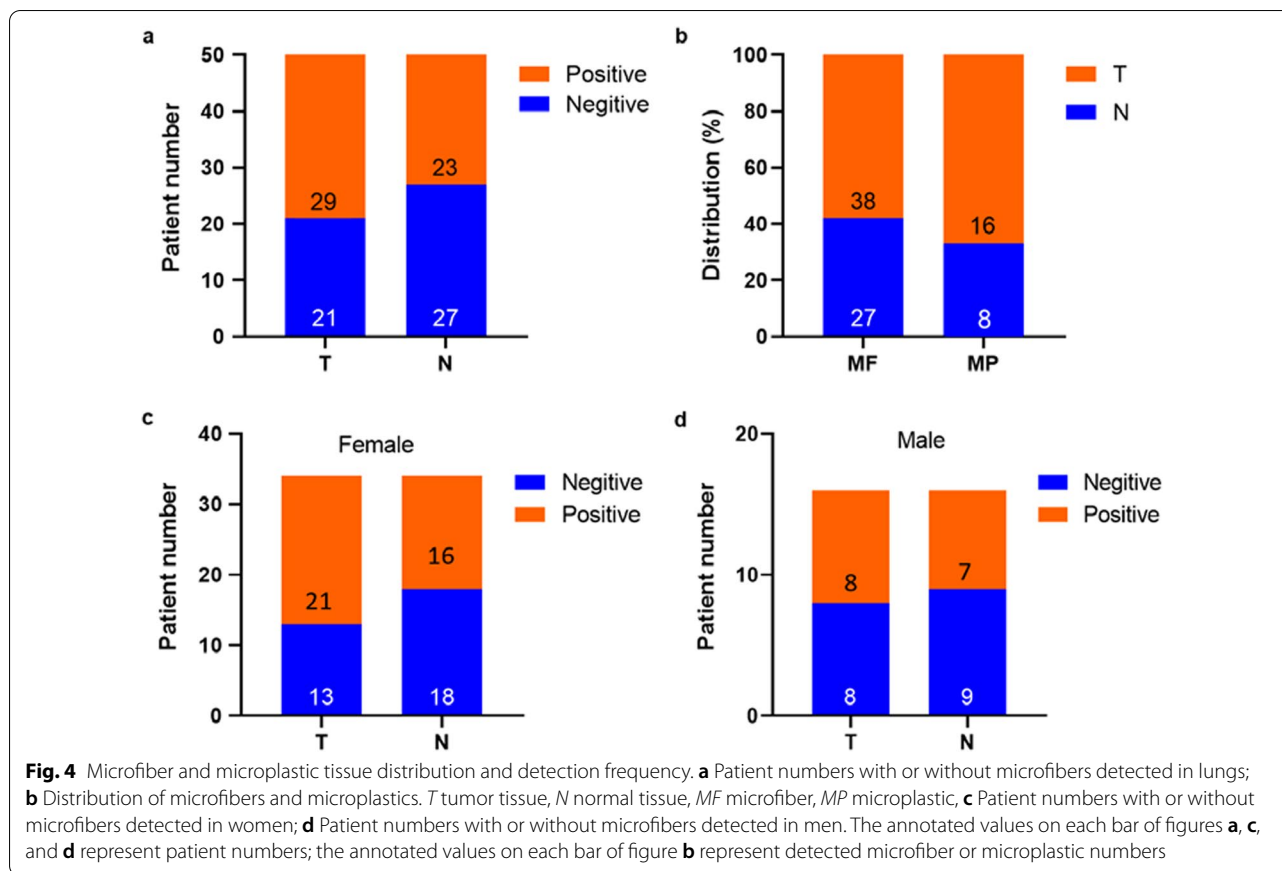


Fig. 3 In situ detection of a cellulose microfiber in the tumor lung tissue slice. **a** the whole tissue section image under Vis spectrum; **b** the whole tissue section image under IR spectrum; **c** microfiber detected under IR spectrum; **d** microfiber detected under Vis spectrum; **e** detected dots with confirmed cellulose composition, the characteristic peak around 1200 cm^{-1} within the red rectangle indicated the composition of cellulose; **f** strong signals (in white color) with the specific cellulose characteristics. Note: Three paired lung tissues (3 normal and 3 tumor tissues) were examined for in situ fibers, but only a single fiber was found in one normal tissue slice

and normal (1.49 ± 0.96 mm) tissues, and the width of microplastics in tumor (34.29 ± 18.60 μm) and normal (34.15 ± 17.91 μm) tissues were quite similar. Moreover, microfibers detected in the lungs were mainly > 1000 μm in length, with 63% for microfiber and 50% for microplastic in tumor tissue, 48% for microfiber and 63% for microplastic in normal tissue (Additional file 1: Figure S1a–b). The width of microfiber mainly falls in < 30 μm in both tumor and normal tissues, accounting for 47.37%

and 51.85%, respectively. However, microplastic widths have the highest proportion of 30–50 μm in tumor tissue, accounting for 56.25%, while the highest proportions of < 30 μm and 30–50 μm in normal tissue are both 37.5% (Additional file 1: Figure S1c–d).

Multiple types of microfibers were detected in the lung. The dominant type of microfibers is cotton which accounts for 39.47% and 51.85% of all detected microfibers in tumor and in normal tissues, respectively. Rayon



ranks the second and constitutes 26.32% and 18.52% of tumor and normal tissues, respectively. The third is polyester, which accounts for 10.53% of tumor and 11.11% of normal tissues. Moreover, 10 kinds of microfibers are detected in tumor, which is more abundant than normal tissues (6 kinds) (Fig. 5b). The colors of microfibers, whether in tumor or normal tissues, are mainly purple and blue with different shades, and a small amount of transparent and yellow microfibers are detected. There are more reddish microfibers in normal tissues (Fig. 5c).

Characterization of microfibers in matched tissues

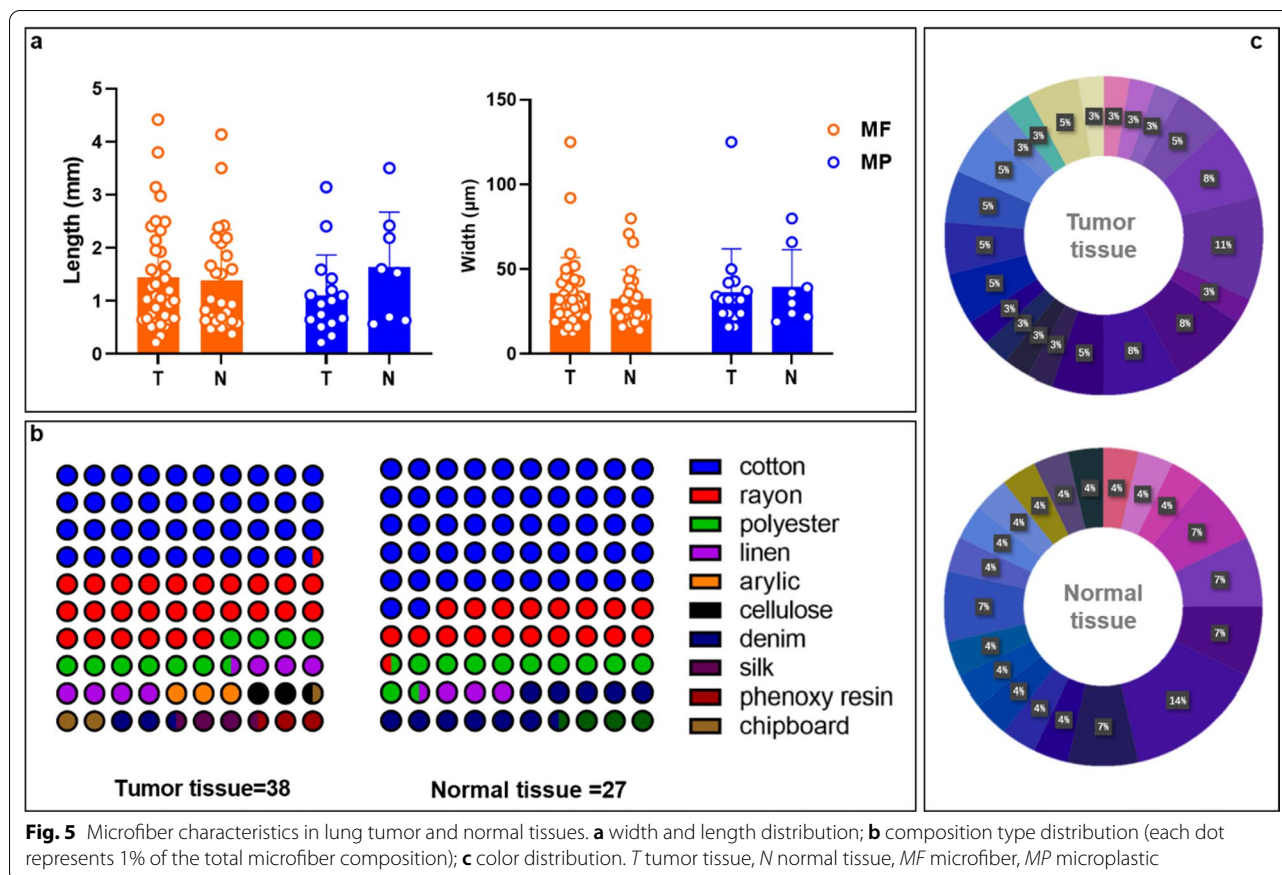
Parameters commonly used to describe the characteristics of microfibers include polymer composition, size, color, density, and shape [40]. To further make clear which characteristic of microfibers may be responsible for the occurrence of GGNs, we also conducted matched samples comparison for the case that microfibers were detected in both tumor and normal tissues of the same patient. The values of width (mean \pm SEM values; $34.29 \pm 18.60 \mu\text{m}$) and length ($1.75 \pm 0.79 \text{ mm}$) in tumor are higher than those in normal tissues by 0.4% ($p=0.981$) and 18.1% ($p=0.381$), respectively (Additional

file 1: Figure S2a). Notably, only one-tenth of the colors and one-third of the fiber composition types are the same in matched tumor and normal tissues (Additional file 1: Figure S2b–c). The types and colors of microfibers in tumor tissues were more abundant than those in normal tissues, which suggests the microfiber sources in tumor tissues may be more diversified.

High risk of microfibers exposure correlates with GGNs

To further study the correlation of microfibers with the occurrence of GGNs, we examined the factors contributing to the accumulation of microfibers in the GGN tumor tissues. Chi-square test revealed that microfibers are more likely to be detected in the tumor tissue if one has a history of high microfiber exposure risk in life or work, when a microfiber detection rate reaches 72.00% (Fig. 6a). However, this phenomenon was not found in the tumor tissue of low microfiber exposure risk, of which the detection rate was 42.11%. This suggests that exposure to microfibers may lead to the accumulation of microfibers in the lung, which finally contributes to the formation of GGNs.

Initially, a sex-specific difference in incidence of lung cancer has been reported; women are more likely



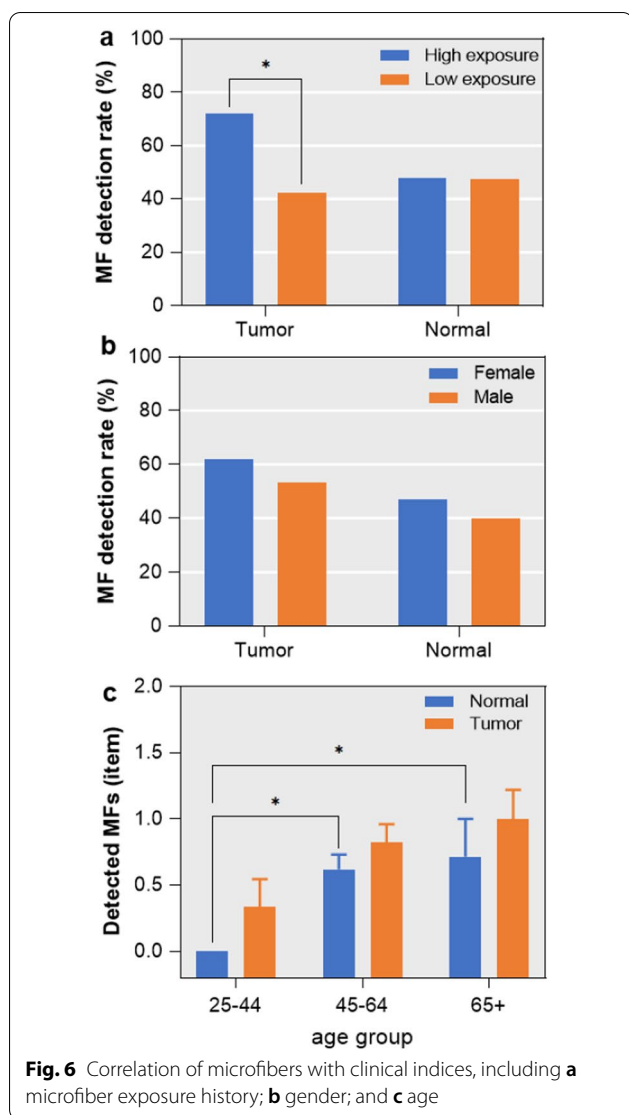
developing GGN [41, 42]. We next examined whether gender is related to the detection rate of microfibers in the tumor or normal tissue of the lung. The microfiber detection rate of the female ($n=34$) in either tumor (61.76%) or normal (47.06%) tissues is higher than that of the male ($n=16$, 53.33% and 40.00%, respectively), but there is no significant detection rate difference between the two genders (Chi-square test, $p=0.482$) (Fig. 6b).

In addition, according to the age classification of lung cancer epidemiology, we found that with the increase of age, the content of microfiber in lung tissue gradually increased (Fig. 6c). Importantly, the amount of microfibers in normal tissue is significantly increased with age (ANOVA, $p<0.05$); the magnitude of microfibers in tumor tissues of patients with GGN also increased with age (Pearson correlation, $p=0.058$) but not significantly different (ANOVA test, $p=0.246$).

Microfibers in lung exhibit high surface roughness

We further characterize the microfibers in human lung tissues by scan electron microscope; the data demonstrate that there are numerous wear and gullies on microfibers as detected by their typical main body structure

(Fig. 7a, c, e) and local surface morphology (Fig. 7b, d, f). Of note, little attention has been paid to the index of surface roughness. This kind of morphology is different from that found in the atmospheric fallout in Shanghai, as we find that there are both worn and unworn microfibers in the air (Additional file 1: Figure S3), which may be related to their aging degree in the environment. Besides, our data confirmed that the sampling, digestion, and identification processes would not be the cause of surface wear (Additional file 1: Figure S4). Of note, microfibers in both tumor and normal tissues exhibited a higher roughness value ($R_a=0.90\pm 0.84\ \mu\text{m}$, and $0.79\pm 0.43\ \mu\text{m}$, respectively) than those in air ($R_a=0.38\pm 0.22\ \mu\text{m}$) ($p=0.183$) (Fig. 7g), and obvious rougher surface of microfibers in lung tissues than that in the air can be observed (Fig. 7h–k). Moreover, energy-dispersive X-ray spectroscopy (EDS) revealed that microfibers isolated in the lung did not harbor obvious heavy metal residues (Additional file 1: Figure S5).



Discussion

The interrogation of the correlation of microplastics with diseases is an emerging field. The presence of microplastics in human tissues, including gastrointestinal tract and placenta [43, 44], has been previously reported. In this study, we provided solid evidence demonstrating the presence of microplastics in human lung tissues. Preliminary data demonstrated a higher detection rate of microplastics in the GGNs compared to the adjacent normal lung tissues. Moreover, the history of exposure to microfibers correlates with the occurrence of GGNs, which implicates an involvement of microfiber exposure in the etiology of GGNs.

High abundance of microfibers in human lung

In our study, we found that the detection rate of microfibers in normal tissue was significantly increased with age; however, the detection rates of microfibers in patients with GGN of all ages are equivalent and high. This phenomenon indicates that microfibers may affect the occurrence of GGN after reaching the cumulative threshold.

The microfibers detected in the lungs mainly ranged from 1000 to 5000 μm in length. This is different from the length distribution of microfibers in mountainous areas or medium-sized cities. For instance, a recent study found only around 11% of atmospheric deposited microfibers ranged $>1000 \mu\text{m}$ collected from a remote mountain catchment (French pyrenees) [45]. In the medium-sized Dongguan city, atmospheric fallout microfibers longer than 1200 μm constituted around 44% [46]. However, our microplastics distribution is close to the atmospheric microplastics distribution in an urban area of Paris, with 49% fell in the range of 1000–5000 μm [47]. This suggests that large cities may have a high proportion of long fibers in the air than medium-sized cities or remote areas. Of note, since our patients come from different cities and rural areas in China, the high percentage of long fibers in lungs may be because the longer inhaled microfibers may be easily entangled in lungs and difficult to be dispelled [17].

In addition to artificial fibrous microplastics, the cotton microfibers occupied a high proportion. As cotton fibers are capable of subjecting to a variety of different forces, such as abrasive wear whose force extent depends on the fiber construction of the yarn or fabric [48], these cotton microfibers should have similar physical effects as microplastics, if the indirect toxic effects of microplastics by releasing additives are not taken into account.

Most of the pulmonary microfibers probably come from indoor or outdoor air exposure, because the types of microfibers in lung tissue are highly similar to those found in the atmospheric fallout [11], with the highest content being cotton, rayon, and polyester. Previous studies have highlighted the presence of synthetic fibers in the lung tissue of workers in the textile industry, showing cases of respiratory irritation [49, 50]. The inhalability of a particle is size and shape dependent, as only the smallest particles below 5 μm and fibrous particles seem to be able to be deposited in the deep lung. Even though most of the bigger particles (inhalable particles) are subjected to mucociliary clearance in the upper airways, some of them can escape this mechanism and also be deposited in the deep lung. These particles (especially the longer fibers) tend to avoid clearance and show extreme durability in physiological fluids, likely persisting and accumulating when breathed in. This may be the reason why the proportion of long fibers ($>1000 \mu\text{m}$) in lung tissue (48–63%,

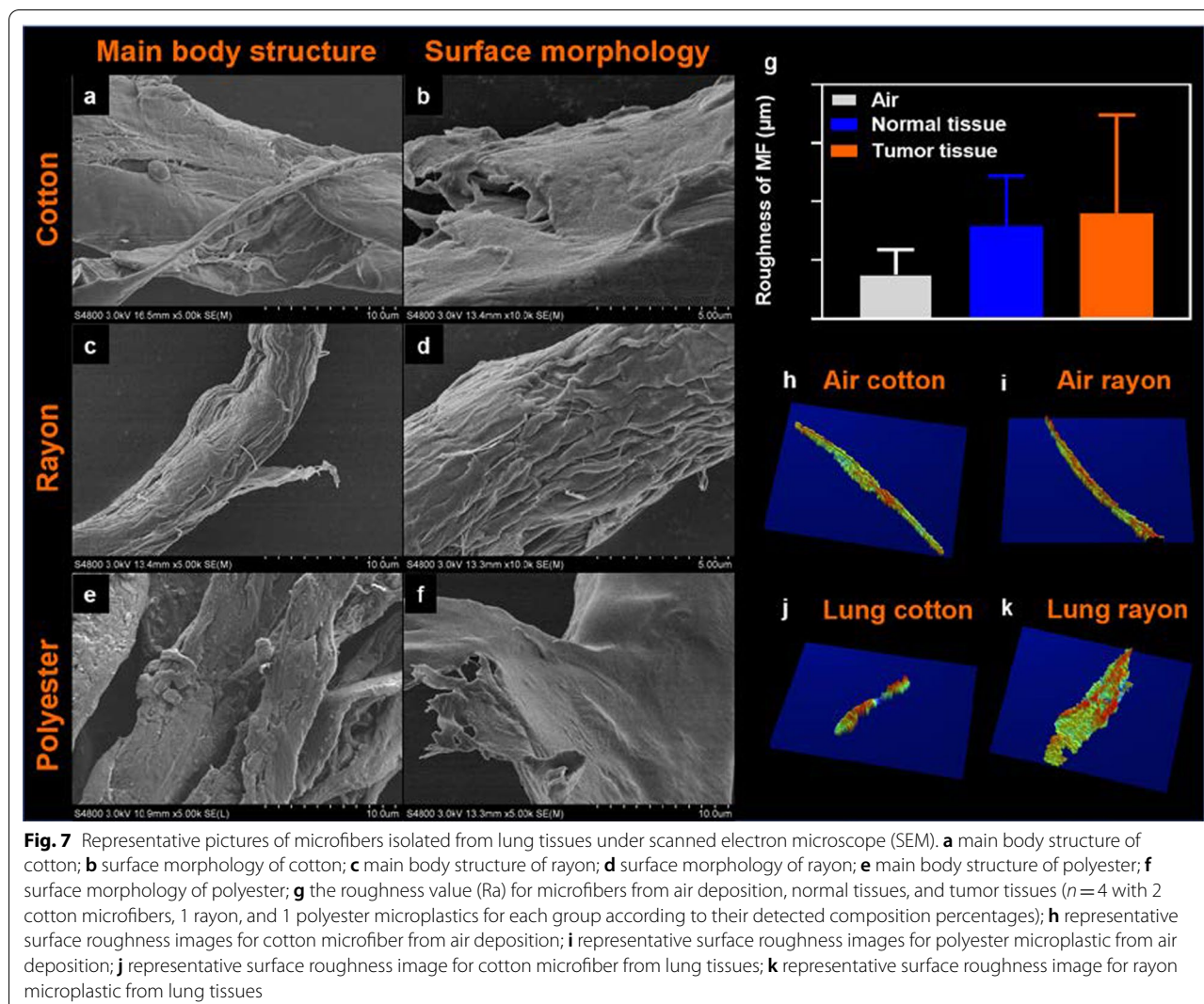


Fig. S1) is much higher than that in urban (44% for $> 1200 \mu\text{m}$) [46] or mountainous air (11% for $> 1000 \mu\text{m}$) [45]. Previous studies report microfiber lengths merely. In this study, we firstly report the microfiber width (or diameter) dimension of microfibers in lung tissues, which is vital factor regulating the deposition of microfibers in the respiratory tract [51].

The morphology of the inhaled fibers (e.g., air pollutants and microplastics) may affect their aerodynamic properties [52, 53], which thereby finally modulate their ability to deposit in the distal pulmonary acinar airways as a result of varied width. Width is the main factor that determines whether or where in the respiratory tract that a microfiber can deposit [51]. Our results suggest that 13–125- μm -wide microfibers/microplastics can reach lung tissues, with a mean width value of $\sim 30 \mu\text{m}$. Once

deposited, fiber length is the main factor that determines whether a microfiber can be effectively cleared [51]. Such elongated fibers (a mean value of $\sim 1.4 \text{ mm}$) tend to align with respiratory airflows, due to higher drag forces that resist sedimentation under gravity, and thus present a special clearance challenge for the lung compared with spheres of equivalent mass [54]. The thin, elongated shape of microfibers also affects clearance rates, enabling microfibers to get entrained into the epithelial layer while inhibiting engulfment by macrophages [51, 55]. Combined with a high surface-to-volume ratio compared to spheres of equivalent mass, such characteristics render non-spherical particles, and fibers in particular, promising candidates to be delivered to the deep lungs, which is supported by the finding that the microfibers identified in the lung are elongated in this study. Furthermore,

we suppose the surface-to-volume ratio, hydrophobicity, size, and other properties of the microfibers can enhance their ability to attach heavy metal, increasing damage to the pulmonary immune microenvironment.

In this study, we have applied three microfiber identification methods, including μ -FTIR, LDIR, and Raman, for different characterization purposes. To quantify the 50 paris lung tissues, we used the μ -FTIR method for $>20\ \mu\text{m}$ items identification [56], because μ -FTIR can quickly provide reliable material composition results in lung tissues.

However, μ -FTIR has its limitations for application, which requires the biological samples to be digested and microfibers should be completely separated before quantification. Thus, to stage the morphological characteristics of microfibers in human lung tissues more intuitively, we prepared extra 6 tissue samples into tissue slices for microfiber in situ observation with LDIR. However, only 3 slices cut from the middle section were used for each sample, as to avoid potential contamination during the process of tissue embedding, and thus, this may underestimate the microfiber abundance in human lung tissues.

Additionally, μ -FTIR has a size limitation, which cannot identify samples smaller than $20\ \mu\text{m}$. Therefore, we tried to use the Raman to figure this problem out, with a lazer wavelength of $785\ \text{nm}$ and was capable of analyzing materials larger than $1\ \mu\text{m}$. However, Raman spectra are particularly vulnerable to biological fluorescence interference [57], and tissue digestion and material separation are still vulnerable. Moreover, there is another important issue needs to be addressed in future studies. The strong laser beam could burn out organic matter and the surface of filter membranes, and even some microfibers (i.e., cotton); and thus, the compositions of some microfibers could not be determined with Raman.

Microfibers and the etiology of GGNs

Generally, when microfibers enter the respiratory system, the lung tissue has two main ways to dispel them. If microfibers deposit on the surface of respiratory mucosa, they can be excreted out of the respiratory tract by coughing or mucociliary escalator [58]. If microfibers reach the alveolar region, macrophages in the alveoli can remove the microfibers through phagocytosis, migration, or lymphatic transportation mechanisms [59]. Macrophages in alveoli often have high clearance efficiency for particles larger than $1\ \mu\text{m}$; thus, microfibers at the micro-sized level are theoretically difficult to remain in lung tissue [60]. However, if the lung is continuously exposed to microfibers for a long time, excessive secretion of chemokines in the lung may be caused, and thus

destroying the normal chemotactic gradient, and may result in macrophages containing ingested microfibers resting in the alveolar space. Or if macrophages engage in “frustrated” phagocytosis for microfibers, digestive enzymes and other cellular contents will be spilled into the alveolar space, and this may mount innate immune responses which drive the sterile inflammation, fibrosis, and other malignancies in the lung [53], which thereby participate in the formation of GGNs and other inflammatory respiratory diseases. The ingestion of microfibers by macrophage may mount innate immune responses which drive the sterile inflammation in the lung, which thereby participate in the formation of GGNs and other inflammatory respiratory diseases. Moreover, the interaction between vitreous particles/fibers and cells may lead to lung inflammation via intracellular messengers and cytotoxic factors which are released, and then cause secondary genotoxicity due to the continuous formation of reactive oxygen species [59, 61].

Increasing evidence demonstrated that microfibers carry bacteria/virus [62], which may play an important role in their interaction with the host. Intriguingly, compared to normal tissue, GGNs harbored a distinct lung bacterial community structure, with significantly increasing Firmicutes and Bacteroidetes [63–65]. Even though there is no report about the biofilm community on airborne microplastics, the biofilm community structures on microplastics are more affected by morphology/surface texture rather than polymer composition [66]. Therefore, we can further perform microbiota analysis on GGNs and normal tissues containing microfibers to reveal the influence of microfiber on the lung microbiota. It is tempting to speculate whether the microbes carried along by microfibers play a role in shaping the specific structure of microbiota in GGN. The microbiota analysis of GGNs and normal tissues that contain or free of microfibers will facilitate to understand the role of microfiber in modulating lung microbiota.

Moreover, airborne microplastic is an ideal vehicle for carrying micropollutants adsorbed to their hydrophobic surface, especially when related to urban environments. Recent studies performed using pre-diagnostic serum samples suggest that environmental exposure to micropollutants plays an important role in the development of a series of cancers, including lung cancer, prostate cancer, breast cancer, liver cancer, and acute myeloid leukemia [67–70]. It is therefore reasonable to speculate that microplastic may affect the occurrence of GGNs by delivering micropollutants, which exerts toxic effect on the host. Of note, in addition to the adsorbed pollutants, microplastics may also contain unreacted monomers, additives, dyes, and pigments which could lead to adverse health effects [71, 72]. However, no heavy metal residue was found here by EDS (Additional file 1: Figure

S6), which may be due to the high detection limit of this method. However, there is no doubt that the high hydrophobicity and adsorption properties of microplastics will lead to the possibility of carrying pollutants into lung tissues, which needs attention in the future.

Surface roughness—a characteristic awaits attention

Parameters commonly used to describe the characteristics of microfibers include polymer composition, size, color, density, shape, etc., whereas little attention is paid to the index of surface roughness. Here we found all microfibers had obvious surface wear in both normal or tumor tissues. This kind of morphology is different from that found in the air, which shows both worn and unworn morphology and may be related to their aging degree in the environment. Although some acidic chemical digestion process may influence the surface of microplastics [73], our pilot experiment confirmed that no obvious surface roughness was caused during the sampling, digestion, and identification processes. Therefore, it is very possible that the surface roughness of microfibers was formed after entering the lungs, formed during microfibers' long-term interaction with the lungs. Some environmental processes, such as mechanical erosion by wind, water, or sand, UV radiation, and biodegradation, will increase the roughness of microplastics [5, 74, 75]. However, there is no report about the increase of roughness after microfibers/microplastics enter tissues. We believe this is the first report of the serious roughness phenomenon of microfibers in human tissues.

Little is known about the consequence of enhanced surface roughness to its interaction with the host. It would be interesting to check whether such characteristic of microfibers modulates its interaction with alveolar macrophages in multiple processes, such as phagocytosis, recognition, and mounting of immune responses. The types of cell death, including apoptosis and necrosis, in response to exogenous stimulation often show distinct effect on the outcome of diseases [76]. It would be fascinating to take the surface roughness as an important characteristic of microfibers into account in studying its role in modulating the fate of macrophages and shaping of the microenvironment, which may constitute a new direction in future research of microfiber–host interaction. The technological advancement in acquisition of nanoscale microfibers will also promote the research on microfiber–host interaction.

Microfibers link pulmonary GGN to occupational disease

Some occupational diseases may be related to long-term exposure to microfibers or microplastics. The “fiber-drawing workers” experienced a statistically significant excess in mortality from lung cancer [49]. Some of the

nylon flock exposed workers had abnormal chest radiographs five-fold than non-exposed ones [50]. In the current study, we found that the microfibers significantly elevated in the normal lung tissues of pulmonary GGN patients with the increase of age. This phenomenon pinpoints the importance of the cumulative threshold of microplastics present in the lung in affecting the occurrence of GGN. Our work also suggests that it is important to perform the routine health examination in those people who have high risk to expose to microplastics, especially in the young people.

Supplementary Information

The online version contains supplementary material available at <https://doi.org/10.1186/s12302-022-00605-3>.

Additional file 1: Table S1. Characteristics of patients. **Table S2.** Clinical information of lung cancer patients. **Figure S1.** Length and width distribution of microfibers and microplastics. **a** the length distribution of microfibers; **b** the width distribution of microfibers; **c** the length distribution of microplastics; **d** the width distribution of microplastics. *MF* microfiber, *MP* microplastic. *T* tumor tissue, *N* normal tissue. **Figure S2.** Microfiber characteristics in matched tumor/normal samples. **a** width and length distribution; **b** color and composition type distribution. *T* tumor tissue, *N* normal tissue. Note: Only patients samples possessing microfibers in both tumor and adjacent normal tissue are included in this figure. **Figure S3.** Representative pictures of airborne cotton and rayon. **a** cotton with smooth surface; **b** cotton with rough surface; **c** rayon with smooth surface; **d** rayon with rough surface. **Figure S4.** Representative pictures of laboratory prepared cotton and rayon microfibers before and after experimental processes (digestion, observation, and identification). **a** cotton before processes; **b** cotton after processes; **c** rayon before processes; **d** rayon after processes. **Figure S5.** Microfiber surficial elemental composition illustrated by SEM/EDS. **a** cotton from a tumor tissue; **b** cotton from a normal tissue; **c** EDS figure for **(a)**; **d** EDS figure for **(b)**; **e** polyester from a tumor tissue; **f** polyester from a normal tissue; **g** EDS figure for **(e)**; **h** EDS figure for **(f)**.

Acknowledgements

The authors thank Jingjing Wang and Jinju Pei (Engineers of the Agilent Technologies, Shanghai, China) for assistance with the in situ detection of microfibers in the lung slice. The authors thank MobiDrop (Zhejiang) Co., Ltd. for their help and support.

Authors' contributions

QC contributed to experimental design, roughness measurement, LDIR measurement together with Agilent Co, data analysis, and writing original draft. JG was involved in clinical samples collection, LDIR measurement together with Agilent Co, data analysis, and original draft writing. HY performed microfiber separation and characterization. HS, YC, and YR were involved in clinical samples collection. YY was involved in SEM/EDS observation and roughness measurement. QZ performed air deposited microfibers collection. HH and HS contributed to manuscript editing. CC performed experimental design. HL contributed to experimental design, data analysis, and original draft writing. All authors read and approved the final manuscript.

Funding

This project was supported by grants from the National Natural Science Foundation of China (42077371 to QC; 81770006 to H.L.) and Shanghai Science and Technology Fund (20S11900600 to C.C.; 19140900600, 22S11900700 and 20dz2210400 to H.L.). H. L. is sponsored by Projects supported by the National Science Foundation for Excellent Young Scholars of China (81922030), Shanghai ShuGuang Program (20SG19).

Availability of data and materials

All data generated or analyzed during this study are included in this published article.

Declarations**Ethics approval and consent to participate**

This study was approved by the Institutional Review Boards of Shanghai Pulmonary Hospital (SPH) (Ethical approval number: K21-020). The detailed approval document is shown in the Supplementary Information.

Consent for publication

Not applicable.

Competing interests

The authors declare no competing interests.

Author details

¹State Key Laboratory of Estuarine and Coastal Research, East China Normal University, Shanghai 200241, China. ²Department of Thoracic Surgery, Shanghai Pulmonary Hospital, Tongji University, Shanghai 200433, China. ³Clinical and Translational Research Center, Shanghai Pulmonary Hospital, Tongji University, Shanghai 200433, China. ⁴Central Laboratory, Shanghai Pulmonary Hospital, Tongji University, Shanghai 200433, China. ⁵Department Evolutionary Ecology and Environmental Toxicology, Goethe University Frankfurt/Main, 60438 Frankfurt/Main, Germany.

Received: 14 November 2021 Accepted: 5 March 2022

Published online: 17 March 2022

References

- Li JY, Liu HH, Chen JP (2018) Microplastics in freshwater systems: a review on occurrence, environmental effects, and methods for microplastics detection. *Water Res* 137:362–374
- Leslie HA et al (2017) Microplastics en route: field measurements in the Dutch river delta and Amsterdam canals, wastewater treatment plants, North Sea sediments and biota. *Environ Int* 101:133–142
- Rochman CM (2018) Microplastics research—from sink to source. *Science* 360(6384):28–29
- Zhang GS, Liu YF (2018) The distribution of microplastics in soil aggregate fractions in southwestern China. *Sci Total Environ* 642:12–20
- Napper I et al (2020) Reaching new heights in plastic pollution—preliminary findings of microplastics on Mount Everest. *One Earth* 3:621–630
- Obbard RW (2018) Microplastics in polar regions: the role of long range transport. *Curr Opin Env Sci Health* 1:24–29
- Ambrosini R et al (2019) First evidence of microplastic contamination in the supraglacial debris of an alpine glacier. *Environ Pollut* 253:297–301
- Galloway TS (2015) Micro- and nano-plastics and human health. *Marine anthropogenic litter*. Springer, Cham, pp 343–366
- Rochman CM et al (2013) Classify plastic waste as hazardous. *Nature* 494(7436):169–171
- Kramm J, Völker C, Wagner M (2018) Superficial or substantial: Why care about microplastics in the anthropocene? *Environ Sci Technol* 52(6):3336–3337
- Zhang Q et al (2020) Microplastic fallout in different indoor environments. *Environ Sci Technol* 54(11):6530–6539
- Zhang Q et al (2020) A review of microplastics in table salt, drinking water, and air: direct human exposure. *Environ Sci Technol* 54(7):3740–3751
- Spasiano D, Pirozzi F (2017) Treatments of asbestos containing wastes. *J Environ Manag* 204:82–91
- Yang X et al (2018) Association between increased small airway obstruction and asbestos exposure in patients with asbestosis. *Clin Respir J* 12(4):1676–1684
- Vianello A et al (2019) Simulating human exposure to indoor airborne microplastics using a Breathing Thermal Manikin. *Sci Rep* 9(1):1–11
- Prata JC et al (2020) Environmental exposure to microplastics: an overview on possible human health effects. *Sci Total Environ* 702:134455
- Pauly JL et al (1998) Inhaled cellulosic and plastic fibers found in human lung tissue. *Cancer Epiderm Biom* 7(5):419–428
- Team NLSTR (2011) Reduced lung-cancer mortality with low-dose computed tomographic screening. *New Engl J Med* 365(5):395–409
- Lee HY, Lee KS (2011) Ground-glass opacity nodules: histopathology, imaging evaluation, and clinical implications. *J Thorac Imag* 26(2):106–118
- Pedersen JH et al (2016) Ground-glass opacity lung nodules in the era of lung cancer CT screening: radiology, pathology, and clinical management. *Oncology* 30(3):266–274
- Fukui T, Mitsudomi T (2010) Small peripheral lung adenocarcinoma: clinicopathological features and surgical treatment. *Surg Today* 40(3):191–198
- Godoy MC, Naidich DP (2009) Subsolid pulmonary nodules and the spectrum of peripheral adenocarcinomas of the lung: recommended interim guidelines for assessment and management. *Radiology* 253(3):606–622
- Ichinose J et al (2014) Invasiveness and malignant potential of pulmonary lesions presenting as pure ground-glass opacities. *Ann Thorac Cardiovas* 20(5):347–352
- Kobayashi Y, Ambrogio C, Mitsudomi T (2018) Ground-glass nodules of the lung in never-smokers and smokers: clinical and genetic insights. *Transl Lung Cancer R* 7(4):487
- Zhang Y et al (2021) Excellent prognosis of patients with invasive lung adenocarcinomas intraoperatively misdiagnosed as AAH/AIS/MIA by frozen section. *Chest* 159(3):1265–1272
- Kim SS, Bharat A (2020) Commentary: video assisted thoracoscopic surgery versus robotic assisted surgery: are we asking the right question? *J Thorac Cardiovas* 160(5):1374–1375
- Meyer M et al (2017) Management of progressive pulmonary nodules found during and outside of CT lung cancer screening studies. *J Thorac Oncol* 12(12):1755–1765
- He Y-T et al (2018) Risk factors for pulmonary nodules in north China: a prospective cohort study. *Lung Cancer* 120:122–129
- Pinsky P, Gierada DS (2020) Long-term cancer risk associated with lung nodules observed on low-dose screening CT scans. *Lung Cancer* 139:179–184
- Lebreton LCM et al (2017) River plastic emissions to the world's oceans. *Nat Commun* 8:15611
- Bai C et al (2016) Evaluation of pulmonary nodules: clinical practice consensus guidelines for Asia. *Chest* 150(4):877–893
- Plastics Europe, *Plastics—The Facts 2020*. An analysis of European plastics production, demand waste data, 2020.p.1-64.
- Whitehouse D (2011) *Handbook of surface and nanometrology*, 2nd edn. CRC, Boca Raton
- Engineer A.S.o.M., ASME B46. 1-2009: *Surface Texture (Surface Roughness, Waviness, and Lay)*. 2009.
- Francisco B et al (2020) Cigarette butts as a microfiber source with a microplastic level of concern. *Sci Total Environ*. <https://doi.org/10.1016/j.scitotenv.2020.144165>
- Catarino AI et al (2018) Low levels of microplastics (MP) in wild mussels indicate that MP ingestion by humans is minimal compared to exposure via household fibres fallout during a meal. *Environ Pollut* 237:675–684
- Singh RP, Mishra S, Das AP (2020) Synthetic microfibers: pollution toxicity and remediation. *Chemosphere* 257:127199
- Lee HJ et al (2012) IASLC/ATS/ERS international multidisciplinary classification of lung adenocarcinoma novel concepts and radiologic implications. *J Thorac Imag* 27(6):340–353
- Asrin NRN, Dipareza A (2019) Microplastics in ambient air (case study: Urip Sumoharjo street and Mayjend Sungkono street of Surabaya City, Indonesia). *IAETSD J Adv Res Appl Sci* 6:54–57
- Chen GL, Feng QY, Wang J (2020) Mini-review of microplastics in the atmosphere and their risks to humans. *Sci Total Environ* 703:135504
- Devesa SS et al (2005) International lung cancer trends by histologic type: male : female differences diminishing and adenocarcinoma rates rising. *Int J Cancer* 117(2):294–299
- Patel JD, Bach PB, Kris MG (2004) Lung cancer in US women: a contemporary epidemic. *JAMA* 291(14):1763–1768
- Schwabl P et al (2019) Detection of various microplastics in human stool: a prospective case series. *Ann Intern Med* 171(7):453–457

44. Ragusa A et al (2021) Plasticenta: first evidence of microplastics in human placenta. *Environ Int* 146:106274
45. Allen S et al (2019) Atmospheric transport and deposition of microplastics in a remote mountain catchment. *Nat Geosci* 12(5):339–344
46. Cai L et al (2017) Characteristic of microplastics in the atmospheric fallout from Dongguan city, China: preliminary research and first evidence. *Environ Sci Pol R* 24(32):24928–24935
47. Dris R et al (2015) Microplastic contamination in an urban area: a case study in Greater Paris. *Environ Chem* 12(5):592–599
48. Hearle JW, Morton WE (2008) *Physical properties of textile fibres*. Elsevier, Amsterdam
49. Hours M et al (2007) Cancer mortality in a synthetic spinning plant in Besançon France. *Occup Environ Med* 64(9):575–581
50. Turcotte SE et al (2013) Flock worker's lung disease: natural history of cases and exposed workers in Kingston Ontario. *Chest* 143(6):1642–1648
51. Donaldson K et al (2011) Identifying the pulmonary hazard of high aspect ratio nanoparticles to enable their safety-by-design. *Nanomedicine* 6(1):143–156
52. Tian L, Ahmadi G (2013) Fiber transport and deposition in human upper tracheobronchial airways. *J Aerosol Sci* 60:1–20
53. Kleinstreuer C, Feng Y (2013) Computational analysis of non-spherical particle transport and deposition in shear flow with application to lung aerosol dynamics—a review. *J Biomech Eng* 135(2):021008
54. Shachar-Berman L et al (2018) Transport of ellipsoid fibers in oscillatory shear flows: implications for aerosol deposition in deep airways. *Eur J Pharm Sci* 113:145–151
55. Chow AH et al (2007) Particle engineering for pulmonary drug delivery. *Pharma Res* 24(3):411–437
56. Chen Y et al (2020) Identification and quantification of microplastics using Fourier-transform infrared spectroscopy: current status and future prospects. *Curr Opin Environ Sci Health* 18:14–19
57. Araujo CF et al (2018) Identification of microplastics using Raman spectroscopy: latest developments and future prospects. *Water Res* 142:426–440
58. Lippmann M, Yeates D, Albert R (1980) Deposition, retention, and clearance of inhaled particles. *Occup Environ Med* 37(4):337–362
59. Tran C et al (2000) Inhalation of poorly soluble particles. II. Influence of particle surface area on inflammation and clearance. *Inhal Toxicol* 12(12):1113–1126
60. Geiser M, Kreyling WG (2010) Deposition and biokinetics of inhaled nanoparticles. *Part Fibre Toxicol* 7(1):1–17
61. Greim H et al (2001) Toxicity of fibers and particles? Report of the workshop held in Munich Germany. *Inhal Toxicol* 13(9):737–754
62. Kim YI et al (2020) Reusable filters augmented with heating microfibers for antibacterial and antiviral sterilization. *ACS Appl Mater Interfaces* 13(1):857–867
63. Liu YH et al (2018) Lung tissue microbial profile in lung cancer is distinct from emphysema. *Am J Cancer Res* 8(9):1775–1787
64. Peters BA et al (2019) The microbiome in lung cancer tissue and recurrence-free survival. *Cancer Epiderm Biomarkers* 28(4):731–740
65. Ren Y et al (2019) Whole genome sequencing revealed microbiome in lung adenocarcinomas presented as ground-glass nodules. *Transl Lung Cancer R* 8(3):235–246
66. Parrish K, Fahrenfeld NL (2019) Microplastic biofilm in fresh- and wastewater as a function of microparticle type and size class. *Environ Sci Wat Res* 5(3):495–505
67. Emeville E et al (2015) Associations of plasma concentrations of dichlorodiphenyldichloroethylene and polychlorinated biphenyls with prostate cancer: a case-control study in Guadeloupe (French West Indies). *Environ Health Persp* 123(4):317–323
68. Engel LS et al (2019) Prediagnostic serum organochlorine insecticide concentrations and primary liver cancer: a case-control study nested within two prospective cohorts. *Int J Cancer* 145(9):2360–2371
69. Koutros S et al (2015) Prediagnostic serum organochlorine concentrations and metastatic prostate cancer: a nested case-control study in the Norwegian Janus serum bank cohort. *Environ Health Persp* 123(9):867–872
70. Park EY et al (2020) Impact of environmental exposure to persistent organic pollutants on lung cancer risk. *Environ Int* 143:105925
71. Gasperi J et al (2018) Microplastics in air: are we breathing it in? *Curr Opin Environ Sci Health* 1:1–5
72. Chen QQ et al (2018) Pollutants in plastics within the North Pacific Sub-tropical Gyre. *Environ Sci Technol* 52(2):446–456
73. Enders K et al (2017) Extraction of microplastic from biota: recommended acidic digestion destroys common plastic polymers. *Ices J Mar Sci* 74(1):326–331
74. Wang JD et al (2017) Microplastics in the surface sediments from the Beijiang River littoral zone: composition, abundance, surface textures and interaction with heavy metals. *Chemosphere* 171:248–258
75. Asamoah BO, Roussey M, Peiponen KE (2020) On optical sensing of surface roughness of flat and curved microplastics in water. *Chemosphere* 254:126789
76. Paludan SR, Reinert LS, Hornung V (2019) DNA-stimulated cell death: implications for host defence, inflammatory diseases and cancer. *Nat Rev Immunol* 19(3):141–153

Publisher's Note

Springer Nature remains neutral with regard to jurisdictional claims in published maps and institutional affiliations.

Submit your manuscript to a SpringerOpen[®] journal and benefit from:

- Convenient online submission
- Rigorous peer review
- Open access: articles freely available online
- High visibility within the field
- Retaining the copyright to your article

Submit your next manuscript at ► [springeropen.com](https://www.springeropen.com)
